J|A|C|S
ARTICLES
Published on Web 09/15/2006

EPR−ENDOR of the Cu(I)NO Complex of Nitrite Reductase

Oleg M. Usov,[§] Yan Sun,[§] Vladimir M. Grigoryants,[§] James P. Shapleigh,[#] and Charles P. Scholes*,[§]

Contribution from the Center for Biochemistry and Biophysics, Department of Chemistry, University at Albany, State University of New York, Albany, New York 12222, and Department of Microbiology, Wing Hall, Cornell University, Ithaca, New York 14853

Received September 7, 2005; E-mail: cps14@albany.edu

Abstract: With limited reductant and nitrite under anaerobic conditions, copper-containing nitrite reductase (NiR) of *Rhodobacter sphaeroides* yielded endogenous NO and the Cu(I)NO derivative of NiR. ^{14}N- and ^{15}N-nitrite substrates gave rise to characteristic ^{14}NO and ^{15}NO EPR hyperfine features indicating NO involvement, and enrichment of NiR with ^{63}Cu isotope caused an EPR line shape change showing copper involvement. A markedly similar Cu(I)NONiR complex was made by anaerobically adding a little endogenous NO gas to reduced protein and immediately freezing. The Cu(I)NONiR signal accounted for 60−90% of the integrated EPR intensity formerly associated with the Type 2 catalytic copper. Analysis of NO and Cu hyperfine couplings and comparison to couplings of inorganic Cu(I)NO model systems indicated ∼50% spin on the N of NO and ∼17% spin on Cu. ENDOR revealed weak nitrogen hyperfine coupling to one or more likely histidine ligands of copper. Although previous crystallography of the conservative I289V mutant had shown no structural change beyond the 289 position, this mutation, which eliminates the Cδ1 methyl of I289, caused the Cu(I)NONiR EPR spectrum to change and proton ENDOR features to be significantly altered. The proton hyperfine coupling that was significantly altered was consistent with a dipolar interaction between the Cδ1 protons of I289 and electron spin on the NO, where the NO would be located 3.0−3.7 Å from these protons. Such a distance positions the NO of Cu(I)NO as an axial ligand to Type 2 Cu(I).

Introduction

Nitrite reductase (NiR) catalyzes the defining reaction of denitrification, which is the one-electron reduction of nitrite to nitric oxide:

$$NO_2^- + 2H^+ + e^- \rightarrow NO + H_2O$$

Copper-containing NiR possesses a Type 2 copper catalytic center, where nitrite is bound and converted to nitric oxide, and a Type 1 copper center, where electrons are accepted and reductively shuttled to the nearby Type 2 copper. NiR is a trimeric protein, for which each subunit contains a Type 1 and a Type 2 copper center. Scheme 1 shows the proximity of the two copper centers, the location of their direct copper ligands, and the location of catalytically important, non-liganding amino acids at the Type 2 center.[1−4] These latter catalytically important amino acids are a highly conserved Asp (Asp129 here) and His (His287 here) which connect through hydrogen bonds to the oxygens of the nitrite substrate for the purpose of substrate orientation when nitrite is bound at Type 2 copper. Additionally, there is a conserved Ile (Ile 289 here) whose bulky side chain occludes and helps define the ligand binding pocket.

Scheme 1. The Locale of the Type 1 Blue-Green Electron-Transfer Center and the Type 2 Catalytic Center in NiR[a]

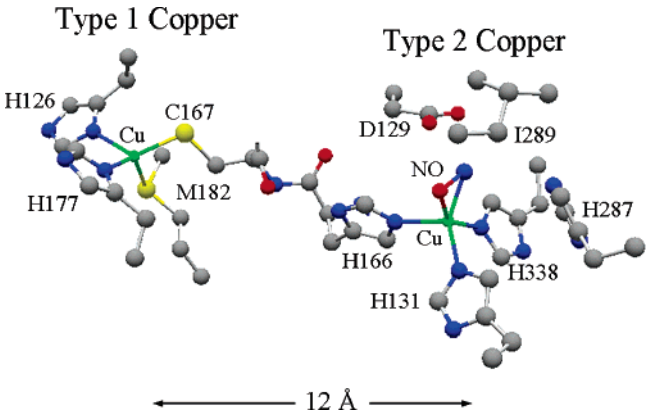

[a] As ligands Type 1 copper has His126, His177, Cys167, and Met182. Type 2 copper has His166, His131, His338, and an axial ligand shown as NO here. Conserved amino acids Asp129, His287, and Ile289 near the Type 2 catalytic center play a critical role in activity. Structure after Tocheva et al.;[5] PDB file 1SNR of NiR from *Alcaligenes faecalis* but with *Rhodobacter sphaeroides* numbers. The *A. faecalis* amino acids His95, His145, Cys136, and Met150 at the Type 1 center respectively correspond to His126, His177, Cys167, and Met182 of *R. sphaeroides*; the *A. faecalis* amino acids His100, His135, His306, Asp98, His255, and Ile257 at the Type 2 center respectively correspond to His131, His166, His338, Asp129, His287, and Ile289 of *R. sphaeroides*.

[§] SUNY at Albany.
[#] Cornell University.

(1) Godden, J. W.; Turley, S.; Teller, D. C.; Adman, E. T.; Liu, M. Y.; Payne, W. J.; LeGall, J. *Science* **1991**, *253*, 438−442.
(2) Adman, E. T.; Godden, J. W.; Turley, S. *J. Biol. Chem.* **1995**, *270*, 27458−27474.
(3) Murphy, M. E. P.; Turley, S.; Kukimoto, M.; Nishiyama, M.; Horinouchi, S.; Sasaki, H.; Tanokura, M.; Adman, E. T. *Biochemistry* **1995**, *34*, 12107−12117.
(4) Murphy, M. E. P.; Turley, S.; Adman, E. T. *J. Biol. Chem.* **1997**, *272*, 28455−28460.
(5) Tocheva, E. I.; Rosell, F. I.; Mauk, A. G.; Murphy, M. E. *Science* **2004**, *304*, 867−870.

10.1021/ja056166n CCC: $33.50

Interest in the mechanism of NiR has extended to understanding what becomes of the NO itself. It has been determined that NiR can be run backward using NO as a substrate to produce nitrite and reducing equivalents.[6] X-ray crystallography has been recently performed on a construct of NiR in which initially reduced NiR was reacted with externally supplied NO gas, and the structure indicated NO to be ligated in a side-on fashion so that both the N and the O were directly bound to the Type 2 copper.[5] On the basis of EPR spectroscopy (not actually performed on the crystals themselves), the adduct was assigned as a cupric complex.[5] In a separate crystallographic study,[7] the side-on coordination of NO to Type 2 copper was observed as one of several axial coordination modes taken by water, nitrite, and NO, even from within the same batch of crystals and even without the addition of exogenous NO.

A nitrogenous biomimetic for NO-bound Type 2 copper of NiR has been prepared under reducing conditions that discriminated it from cupric copper, and it was definitively characterized: first, by EPR as a paramagnetic Cu(I)NO complex showing electron spin density on Cu and NO, and second, by X-ray crystallography that indicated nitrogen end-on binding of the NO to Cu(I).[8] Recent modeling and density functional theory (DFT) studies on NO at the active site of Type 2 copper in NiR have pointed to a stable paramagnetic $S = {}^1/_2$ {CuNO}[11] oxidation level having a Cu(I)−NO$^{\bullet}$ configuration with ∼90% of the spin on the NO and ∼10% on the Cu;[9] the conformation of this NO when oriented for side-on copper ligation was predicted to be marginally more stable than the end-on form bound through N.

The mechanism and underlying structure of cupric NiR have been previously studied through application of electron nuclear double resonance (ENDOR).[10−12] Recent studies upon wild-type and mutant forms of NiR combined enzymatic measurements with ENDOR; they detected exchangeable proton features associated with the Asp129 and His287 (shown in Scheme 1) and correlated changes in these proton features with loss of enzymatic activity.[12] These critical Asp and His side chains determined the location of protons that would hydrogen bond to a nitrite oxygen and facilitate conversion of nitrite to NO and water upon reduction.[12] Mutation of I289 to V289 caused minor perturbation to enzyme activity, but the I289V mutation allowed binding to the Type 2 copper of a small molecule, formate, whose proton features were detected by ENDOR.[12] Such formate binding was not observed with wild-type protein, and we suggested that at least one purpose of I289 was to block unwanted binding of small molecules other than water and nitrite within the Type 2 copper pocket. Subsequent X-ray study on the *Alcaligenes faecalis* homologue of the *Rhodobacter sphaeroides* I289V mutant indicated that "no global structure rearrangement had resulted from the mutation" and that the "positions of the side chains of the active site residues that lay within 8 Å of the copper (with the exception of the isoleucine itself) were equally well conserved conformationally".[13] In addition, the enzyme activity was actually slightly larger for the I289V mutant.[13] Thus, for the I289V mutant there is only local perturbation to enzyme structure from the mutation and a slight increase in NiR activity, whereas for the I289A mutant there is more perturbation to structure and a decrease in enzyme activity.[13]

Over the past 30 years, a considerable literature of spectroscopic,[14,15] crystallographic,[16] and theoretical[17] understanding has emerged on heme−NO systems. Over the past 10 years, NO has gained intrinsic interest as a small molecule of signaling and sensing, for example, in soluble guanylate cyclase.[18] A heme-containing nitrite reductase generates NO for the metabolism of *Pseudomonas aeruginosa*.[19] In ref 20, we used EPR and nitrogen and proton ENDOR to probe the electronic structure of NO-bound cytochrome *c*′ of *R. sphaeroides* 2.4.3. We determined electronic evidence of spin density on the NO of a heme protein whose function, when reduced, is to transport and store NO[21,22] in the same *R. sphaeroides* organism where NiR produces the NO.

There is not, at this time, the spectroscopic, crystallographic, and theoretical underpinning for copper−NO complexes that there is for heme−NO systems. NiR is an unusual enzyme whose purpose in the metabolism of the denitrifying bacteria is to produce large amounts of NO. Binding of NO to the very Type 2 copper catalytic site that produces the NO in the first place is unprecedented, even if the NO binding that we observe turns out to be product inhibition. Furthermore, the enzyme has been made to run in reverse by binding NO to create nitrite and reducing equivalents. For an NO complex of the same copper protein which catalytically produces NO in large quantities, a motivation for this present work is to provide spectroscopic underpinnings on the local metallo−NO electronic structure. We do this for comparison with the theoretical predictions on the electronic structure and spin distribution in model Cu(I)NO complexes[9] and for comparison with the spectroscopic and crystallographic results of biomimetic Cu(I)-NO complexes.[8]

Materials and Methods

Materials. Using the plasmid pET17b-*nirK*, which contains ampicillin resistance and the *Nir* gene, overexpression, purification, activity, and copper content assay of wild-type NiR and its I289V and I289A mutants were carried out as described previously.[12] Following overexpression of NiR, the protocol was to add ∼1 mL of 0.1 M $CuCl_2$ to the supernatant containing Cu-free NiR in order to replenish the copper in the NiR.[23] For preparation of NiR with isotopic enrichment, $^{63}CuCl_2$ (99.8% in ^{63}Cu from Isotec, Inc.) was used. (Natural abundance Cu

(6) Wijma, H. J.; Canters, G. W.; de Vries, S.; Verbeet, M. P. *Biochemistry* **2004**, *43*, 10467−10474.
(7) Antonyuk, S. V.; Strange, R. W.; Sawers, G.; Eady, R. R.; Hasnain, S. S. *Proc. Natl. Acad. Sci. U.S.A.* **2005**, *102*, 12041−12046.
(8) Ruggiero, C. E.; Carrier, S. M.; Antholine, W. E.; Whittaker, J. W.; Cramer, C. J.; Tolman, W. B. *J. Am. Chem. Soc*. **1993**, *115*, 11285−11298.
(9) Wasbotten, I. H.; Ghosh, A. *J. Am. Chem. Soc.* **2005**, *127*, 15384−15385.
(10) Howes, B. D.; Abraham, Z. H. L.; Lowe, D. J.; Bruser, T.; Eady, R. R.; Smith, B. E. *Biochemistry* **1994**, *33*, 3171−3177.
(11) Veselov, A.; Olesen, K.; Sienkiewicz, A.; Shapleigh, J. P.; Scholes, C. P. *Biochemistry* **1998**, *37*, 6095−6105.
(12) Zhao, Y.; Lukoyanov, D. A.; Toropov, Y. V.; Wu, K.; Shapleigh, J. P.; Scholes, C. P. *Biochemistry* **2002**, *41*, 7464−7474.
(13) Boulanger, M. J.; Murphy, M. E. *Protein. Sci.* **2003**, *12*, 248−256.
(14) Dickinson, L. C.; Chien, J. C. *J. Am. Chem. Soc.* **1971**, *93*, 5036−5040.
(15) Yonetani, T.; Yamamoto, H.; Erman, J. E.; Leigh, J. S., Jr.; Reed, G. H. *J. Biol. Chem.* **1972**, *247*, 2447−2455.
(16) Scheidt, W. R.; Piciulo, P. L. *J. Am. Chem. Soc.* **1976**, *98*, 1913−1919.
(17) Zhang, Y.; Gossman, W.; Oldfield, E. *J. Am. Chem. Soc.* **2003**, *125*, 16387−16396.
(18) Denninger, J. W.; Marletta, M. A. *Biochim. Biophys. Acta* **1999**, *1411*, 334−350.
(19) Silvestrini, M. C.; Tordi, M. G.; Musci, G.; Brunori, M. *J. Biol. Chem.* **1990**, *265*, 11783−11787.
(20) Usov, O. M.; Choi, P. S.-T.; Shapleigh, J. P.; Scholes, C. P. *J. Am. Chem. Soc.* **2006**, *128*, 5021−5032.
(21) Mayburd, A. L.; Kassner, R. J. *Biochemistry* **2002**, *41*, 11582−11591.
(22) Choi, P. S.; Grigoryants, V. M.; Abruna, H. D.; Scholes, C. P.; Shapleigh, J. P. *J. Bacteriol.* **2005**, *187*, 4077−4085.
(23) Olesen, K.; Veselov, A.; Zhao, Y.; Wang, Y.; Danner, B.; Scholes, C. P.; Shapleigh, J. P. *Biochemistry* **1998**, *37*, 6086−6094.

contains 69% ^{63}Cu and 31% ^{65}Cu. ^{65}Cu and ^{63}Cu both have the same $I = {}^3/_2$ nuclear spin state, and ^{65}Cu has a magnetic moment which is about 8% higher than that of ^{63}Cu.) Samples to be deuterated were exchanged and concentrated twice with a microfuge concentrator (Microcon) versus D_2O (99.9% isotopic enrichment, Cambridge Isotopes Laboratory, CIL) buffer at pD 7 to give an approximate 95% D_2O enrichment; for these samples, perdeuterated glycerol (CIL) was used as a glassing agent.[12,24]

Methods. (a) Sample Preparation. For most of the spectra reported here, a method was used which enzymatically generated endogenous NO within the small volume of the reduced, deaerated sample. In this method, NiR samples having a subunit concentration of 0.5 mM, 50 mM pH 7.2 phosphate buffer, a 2-fold molar excess of nitrite, 40% glycerol (for rapid freezing), and 10 μM phenazine methosulfate (PMS, Sigma) mediator were first deaerated by argon exchange for 5 min with gentle agitation under a continuously flowing, scrubbed argon atmosphere in a 7 mL septum vial.[25] Samples were then transferred by an argon-flushed Hamilton gastight syringe to argon-flushed EPR tubes (3.0 mm i.d., 4.0 mm o.d. tubes for X-band EPR; 2.0 mm i.d., 2.4 mm o.d. tubes for Q-band ENDOR). A 2-fold molar excess of deaerated, argon-exchanged NADH (Sigma) reductant was added by Hamilton gastight syringe and thoroughly mixed by the Hamilton needle tip within the EPR tube for ~1 min until the sample bleached. This is the stage where enzymatically produced NO would be released by NiR itself. Samples were rapidly frozen by plunging into liquid nitrogen as the EPR tube above the sample was continuously flushed with argon. The X-band samples were ~0.2 mL in volume, and the Q-band samples were ~0.05 mL in volume. Samples were prepared with ^{14}N-nitrite ($^{14}NO_2^-$, Sigma) and ^{15}N-nitrite ($^{15}NO_2^-$, 98% isotopic enrichment, CIL). A different method, using a small amount of exogenous NO, also provided a signal markedly similar to that obtained from NO generated endogenously by enzyme action. With this method, we carefully reduced our argon-exchanged, deaerated sample by using a 2-fold excess of NADH within the EPR tube under argon, bubbled into it a small (~50 μL) aliquot of freshly scrubbed NO gas, and quickly froze the sample within ~1 min of the introduction of NO. The EPR signal, which is shown in Figure 1C, was remarkably similar to the EPR signal (Figure 1A) produced by endogenous production of NO.

The methods which Tocheva et al.[5] used to generate diffraction-quality crystals with a Cu(II) species as the final product had employed long exposure to exogenous NO. Tocheva et al.[5] also generated EPR signals from liquid samples of reduced NiR subject to long incubation of up to 20 min under exogenous NO. When we reduced our sample within a 7 mL vial under argon, added several milliliters of scrubbed NO (^{14}NO, 99% purity, Air Products), and then after a 5 min incubation transferred the sample anaerobically to the EPR tube where the sample was frozen, we obtained a Cu(II) signal similar to that reported by Tocheva et al.[5] This signal is shown in Figure 1D. In our own efforts, we found that details of the cupric Type 2 complex changed over the period of NO incubation, possibly because of the re-emergence of resting cupric NiR, as reported by Tocheva et al. in their Supporting Information.[5]

(b) X- and Q-Band EPR. X-band EPR (9.52 GHz) was carried out with an ER-200 IBM Bruker X-band spectrometer equipped with a standard TE_{102} EPR cavity and an APD Cryogenics LTR-3 Helitran system (Allentown, PA) operated at 15 K. X-band EPR data were collected in a personal computer using the EW Software routines (Scientific Software Sales, Plymouth, MI). The program SIMPIPM was used for fitting of EPR spectra to obtain estimates of hyperfine couplings and g-values.[26] The Q-band EPR (34.1 GHz) system operates below 2 K with pumped helium and is generally used in a dispersion, rapid passage mode because the dispersion, rapid passage signal is highly sensitive to nuclear spin transitions of the ENDOR process. Dispersion, rapid passage EPR signals with slow electron spin relaxation have the appearance of inverted absorption signals, although spin relaxation can cause distortion of the rapid passage line shape. An EPR signal with the apparent line shape of a standard first derivative absorption EPR signal can be obtained by numerically taking a first derivative of the rapid passage signal.

Q-band ENDOR measurements were performed under dispersion (χ'), rapid passage field-modulated conditions at 2 K with the cryogenically tunable TE_{011} Q-band resonator,[27] as previously reported.[11,12,28] In doing ENDOR, we monitor the radio frequency (RF)-induced change in the rapid passage, 100 kHz field-modulated dispersion EPR signal as we sweep the frequency of the RF field.

(c) ENDOR Theory: Protons. The frequencies of proton ENDOR features, $^{\mathrm{P}}\nu_{\mathrm{ENDOR}}$, center to first order at the free proton nuclear Zeeman frequency, ν^{P}. Taking A as the hyperfine coupling, one finds the proton frequencies are split away from ν^{P} by $\pm{}^1/_2$ A for protons coupled to the electron spin $^1/_2$ doublet.[12,20,24] Proton ENDOR frequencies, occurring as "+" or as "−" Zeeman branches, are[29]

$$^{\mathrm{P}}\nu^{\pm}_{\mathrm{ENDOR}} = |\nu^{\mathrm{P}} \pm A/2| \tag{1}$$

First-order expresions hold when $\nu^{\mathrm{P}} \gg A/2$, as is the case here with a magnetic field of ~1.2 T and ν^{P} in the 50 MHz range. Detailed descriptions of the proton hyperfine tensor and dipolar contributions to it are provided in the Methods Sections of refs 20 and 24.

Distant protons such as those on I289 typically have only dipolar couplings. The point dipolar couplings, A_{Dip}, of protons coupled to electron spin localized at a particular center would be[24]

$$A_{\mathrm{Dip}} = \{f g_{\mathrm{eff}} g_{\mathrm{n}} \beta_{\mathrm{e}} \beta_n / hR^3\}(3\cos^2\theta - 1) = A_{\mathrm{Dip}}(3\cos^2\theta - 1)$$
$$= (39.5 f g_{\mathrm{eff}}/R^3)(3\cos^2\theta - 1)\ (\mathrm{MHz}) \tag{2}$$

where f is the fraction of an unpaired electron on a particular center, g_{eff} is the electronic g-value where the dipolar coupling is measured, g_{n} is the nuclear g-value (= 5.585 for a proton), R is the distance from the proton to the localized center of electron spin, and θ is the angle between the vector **R** and the external magnetic field. The point dipolar Hamiltonian will be axial with respect to the **R** direction. The turning points in the powder ENDOR spectra occurring where $\theta = 0°$ or 90° typically provide the best resolved ENDOR, and the 90° turning point is spatially the most likely.[29]

(d) Nitrogen ENDOR. The first-order expressions for spin 1 ^{14}N ENDOR frequencies of heme, histidine, and NO are

$$^{14}\nu^{+}_{\mathrm{ENDOR}} = |^{14}A/2 \pm {}^3/_2 P + {}^{14}\nu| \quad \text{and} \quad {}^{14}\nu^{-}_{\mathrm{ENDOR}} = |^{14}\mathrm{A}/2 \pm {}^3/_2 P - {}^{14}\nu| \tag{3}$$

where ^{14}A is the hyperfine coupling, P is the quadrupolar coupling, and $^{14}\nu$ (= 3.75 MHz at 1.218 T) is the ^{14}N nuclear Zeeman frequency. (If quadrupolar splitting is resolved, the quadrupolar splitting will be $3|P|$.) The $^{14}\nu^{+}_{\mathrm{ENDOR}}$ branch is often the only one observable with rapid

(24) Usov, O. M.; Choi, P. S.-T.; Shapleigh, J. P.; Scholes, C. P. *J. Am. Chem. Soc.* **2005**, *127*, 9485−9494.

(25) Three cycles of freeze−pump−thaw were also tried for rigorous removal of oxygen. Freeze−pump−thaw gave Cu(I)NONiR spectra essentially unchanged from those obtained by the argon-exchange method described in the Methods section that did not involve repetitive freezing of enzyme. A sample was also prepared with no attempt to remove oxygen from solution, and its Cu(I)NONiR features were very similar to those of the anaerobic samples; however, it also gave evidence for oxidized cupric copper.

(26) SIMPIPM is an extension of PIP, which is an extension of QPOW. Nilges, M. J.; Belford, R. L.; Francesconi, L. C. Simulation of strain in EPR spectra using the method of gradients. Presented at the 40th Rocky Mountain Conference on Analytical Chemistry, Denver, CO, July 1998. For QPOW, see: Nilges, M. J. Thesis, University of Illinois, Urbana, 1979.

(27) Sienkiewicz, A.; Smith, B. G.; Veselov, A.; Scholes, C. P. *Rev. Sci. Instrum.* **1996**, *67*, 2134−2138.

(28) Veselov, A. V.; Osborne, J. P.; Gennis, R. B.; Scholes, C. P. *J. Am. Chem. Soc.* **2000**, *122*, 8712−8716.

(29) Hoffman, B. M.; DeRose, V. J.; Doan, P. E.; Gurbiel, R. J.; Houseman, A. L. P.; Telser, J. In *Biological Magnetic Resonance, Vol. 13: EMR of Paramagnetic Molecules*; Berliner, L. J., Reuben, J., Eds.; Plenum: New York, 1993.

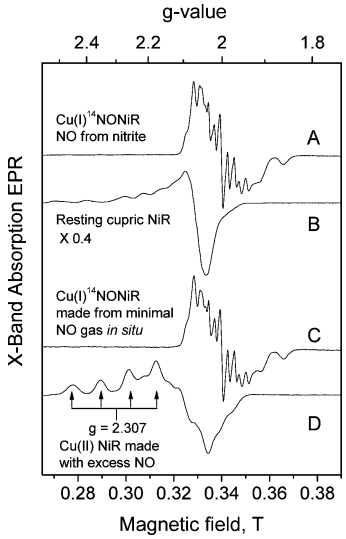

Figure 1. X-band EPR spectra of (A) Cu(I)^{14}NONiR with NO derived enzymatically from ^{14}N-nitrite, (B) resting cupric NiR (signal multiplied by 0.4), (C) Cu(I)^{14}NONiR prepared from reduced NiR by injecting ~50 μL of NO gas into the anaerobic sample, and (D) Cu(II)NiR made from reduced NiR and excess exogenous NO with ~5 min incubation. The splitting between the Cu hyperfine features centered at $g = 2.307$ is 115 G. All samples were from wild-type NiR, 0.5 mM in NiR subunits, with Cu in natural isotopic abundance. The spectra were recorded at $T = 15$ K, 0.6 mT field modulation, 100 s signal averaging over a 0.140 T sweep, 2 mW microwave power, EPR frequency = 9.525 GHz.

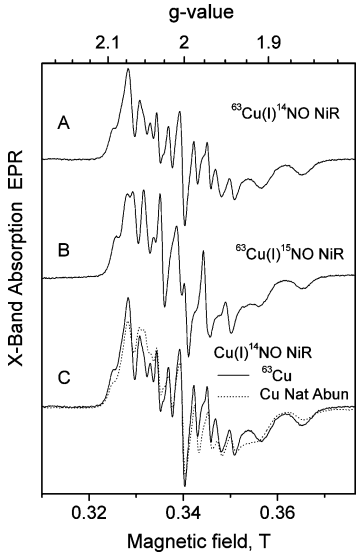

Figure 2. X-band EPR spectra of (A) ^{63}Cu(I)^{14}NONiR prepared from ^{14}N-nitrite and (B) ^{63}Cu(I)^{15}NO NiR prepared with ^{15}N-nitrite. The purpose is show that NO originating from nitrite contributes to the EPR signal. Spectra C provide an overlay of 99% ^{63}Cu-enriched ^{63}Cu(I)^{14}NONiR (solid line) with Cu(I)NONiR containing ^{63}Cu:^{65}Cu in the natural isotopic 69:31 ratio (dotted line). These spectra were recorded at $T = 15$ K, 0.3 mT field modulation, 100 s signal averaging with a 0.070 T sweep, 2 mW microwave power, EPR frequency = 9.525 GHz.

passage Q-band ENDOR for nitrogen features from heme and histidine with couplings less than 30 MHz.[24,28]

Results

Characterization of the Cu(I)NONiR Complex Resulting from the Reaction of Reduced NiR with NO. Figure 1 provides a comparison of the X-band EPR spectrum (1A) of NiR reduced in the presence of ^{14}N-nitrite to the spectrum (1B) of oxidized, resting wild-type NiR, which has both a cupric Type 1 and Type 2 center. The samples for spectra 1A and 1B were from the same enzyme preparation and were equal in concentration. Spectrum 1A, unlike Cu(II) EPR spectra but like those of the {CuNO}^{11} models,[8] showed considerable hyperfine detail near $g = 2.00$ and features whose g-values were less than 2.00. These latter features show Cu hyperfine coupling. Spectrum 1A, again unlike Cu(II) EPR spectra but like those of the {CuNO}^{11} models,[8] could only be observed below liquid nitrogen temperature because of its fast spin relaxation. A double integration of the signal from NiR reduced in the presence of nitrite, and a comparison of that double integral to the double integral of the original resting cupric NiR signal, indicated that spectrum 1A accounted for 30−45% of the integrated intensity of the total resting cupric signals from Type 1 and Type 2 copper in spectrum 1B. If the signal from the NiR reduced in the presence of nitrite arises from a Type 2 copper center, the implication is that a spin count of 60−90% of the available Type 2 copper centers of NiR is providing that signal. Integration of the biomimetic model Cu(I)NO EPR signals reported in ref 8 indicated that {CuNO}^{11} signals from the model corresponded to about ~70% of the available copper. Spectrum 1C is the EPR spectrum of reduced NiR to which a small volume of exogenous NO gas was anaerobically added directly in situ with subsequent quick freezing. Spectrum 1C shows that a reduced NiR sample protected under argon will initially bind NO so as to give an EPR signal remarkably similar to that obtained when reduced NiR reacts with its own nitrite-derived NO. We focus the work reported here on the initially bound NO species, which we characterize in this paper and beyond this point designate as Cu(I)NONiR. A markedly different spectrum is shown in Figure 1D from a sample which was obtained by reacting reduced NiR for ~5 min with a large volume excess of exogenous NO, as described in the Materials section, before transferring the sample to the EPR tube and freezing. This species cannot be the initial EPR species from the reaction of NO with reduced NiR since we have already seen in spectra 1A and 1C that there is an earlier species, viz. Cu(I)NONiR, prepared by two separate methods. Spectrum 1D showed cupric character with well-resolved large copper hyperfine coupling having $A_{||} = 115$ G and $g_{||} = 2.307$, similar to that reported by Tocheva et al.[5] This Cu(II)NO construct, like that reported by Tocheva et al.,[5] has g-values and hyperfine spectra (Figure 1D) different from those of the Cu(I)NONiR complex. Our work focuses on Cu(I)NONiR prepared by enzymatic action of NiR under anaerobic conditions in a small, anaerobically isolated volume with limited, biologically relevant reductant and limited nitrite. These limited reducing and nitrite conditions are plausible conditions that would be encountered when NiR is producing or consuming[6] its own NO.

The spectra shown in Figure 2A,B are the X-band first derivative EPR spectra of ^{63}Cu-enriched NiR reduced respectively in the presence of ^{14}N-nitrite (A) and ^{15}N-nitrite (B). The difference between ^{14}N and ^{15}N isotopes is evident in the details of hyperfine structure, especially near $g = 2.00$, and the implication is that NO originating from nitrite contributes to the EPR signal. Spectrum 2C overlays the spectra of Cu(I)^{14}NONiR samples prepared from ^{63}Cu-enriched (solid) and naturally abundant copper (dotted). Given the magnetic similarity of the ^{63}Cu and ^{65}Cu isotopes, the spectral differences between samples with natural abundance Cu and with enriched

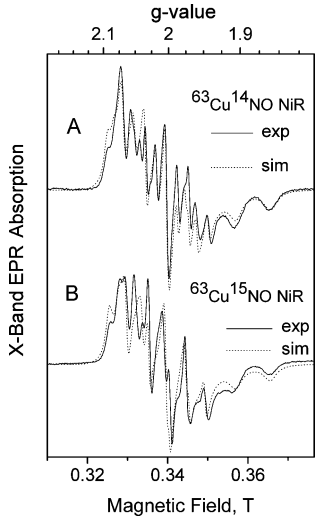

Figure 3. Comparison of the experimental X-band absorption first derivative signals (solid line) to simulations (dotted line) for (A) ^{63}Cu(I)^{14}NONiR and (B) ^{63}Cu(I)^{15}NONiR. The experimental spectra are those of Figure 2A,B. The spectra were computed using the program SIMPIPM.[26] The following parameters (hyperfine couplings in Gauss) were used for simulation: $g_x = 2.046$, $g_y = 1.998$, $g_z = 1.926$, $^{Cu}A_x = 37$, $^{Cu}A_y = 44$, $^{Cu}A_z = 88$, $^{14N}A_x = 17$, $^{14N}A_y = 29$, $^{15N}A_x = 24$, $^{15N}A_y = 40$, $^{14}A_z$ and $^{15}A_z < 10$ G. The principal directions for $^{Cu}A_y$ and $^{Cu}A_z$ are respectively rotated by 20° in the $y-z$ plane away from the principal directions for g_y and g_z. Gaussian line widths (in Gauss) between derivative extrema are $W_x = 30$, $W_y = 13$, and $W_z = 52$.

^{63}Cu are not large, but the EPR features are sharper in the presence of enriched ^{63}Cu. This spectral difference indicates that Cu must be involved with the signal originating from NiR that has been reduced in the presence of nitrite, thus providing an additional rationale for calling the signal Cu(I)NONiR. The Q-band spectrum of Cu^{14}NONiR obtained by dispersion, rapid passage EPR at 1.8 K is shown in the Supporting Information, Figure 1S. Although the passage signal was broader than the X-band spectra and showed distortion at its low-field extremum, the derivative of this spectrum provided additional confirmation of g-values, which were estimated as $g_x = 2.044 \pm 0.003$, $g_y = 1.998 \pm 0.002$, and $g_z = 1.923 \pm 0.005$, and evidence near g_z for Cu hyperfine broadening.

Simulations (Figure 3) were performed on the X-band spectra for both ^{63}Cu(I)^{14}NONiR and ^{63}Cu(I)^{15}NONiR. The major parameters used in fitting these spectra were the electronic **g**-tensor of the complex, the ^{63}Cu hyperfine tensor, and the ^{14}NO and ^{15}NO nitrogen hyperfine tensors. The detailed hyperfine and g-value parameters from the simulations are provided in Table 1 and are compared there to the parameters of the other known {Cu(I)NO}^{11} complexes with nitrogenous ligands[8] and in zeolites.[30,31] The simulations show the high-field features having copper hyperfine structure in the vicinity of $g = 1.9$ that are associated with g_z, the overlapping nitrogen and copper structure in the $g = 2.00$ region that is associated with g_y, and the low-field features that are associated with g_x. A better fit of simulation to experimental spectra, judged by a diminished sum of squared residuals, was obtained if the principal directions for $^{Cu}A_y$ and $^{Cu}A_z$ were respectively rotated by 20° in the $y-z$ plane away from the principal directions for g_y and g_z. There appears to be a small free radical contribution (<1% of the overall signal) at $g = 2.00$; the contribution possibly is from the reductant. The major location where simulations and experimental spectra did not fit was near 0.332 T. The fit could be improved by considering two species differing by approximately 0.03 unit in their g_x values. An implication of two species is that there may be slightly different conformations of the Cu(I)NONiR complex, as have been found for zeolite Cu(I)-NO complexes.[31] We provide in Figure 2S in the Supporting Information comparisons of the EPR spectra of the Cu(I)^{14}NONiR and Cu(I)^{15}NONiR to the corresponding model {Cu(I)NO}^{11} derivatives reported by Ruggiero et al.[8] There are similarities between the hyperfine patterns of Cu(I)NONiR and the hyperfine patterns of the model biomimetic {Cu(I)NO}^{11} derivatives near $g = 2.00$, although the copper hyperfine couplings are larger for the model; the {Cu(I)NO}^{11} model shows a smaller g_z.

Because EPR is most effective at resolving relatively large hyperfine couplings, we used ENDOR to resolve weaker nitrogen couplings. As an example of such weak nitrogen couplings, we have reported weak couplings with magnitude ~6 MHz from heme nitrogens of the NO complex of heme.[20] We believed that there was the potential, given the likely nitrogenous ligands of the Cu, to find such weak couplings to nitrogen ligands of the copper, most likely to histidine nitrogen. The ENDOR feature observed (Figure 4) had a frequency of 7.5 MHz and was not altered when NiR was reduced in the presence of ^{14}N versus ^{15}N nitrite. Its frequency stayed at approximately the same frequency across the EPR line of Cu(I)-NONiR. In the absence of deuterium, there are no naturally occurring nuclei other than ^{14}N-nitrogen which will provide hyperfine features in this frequency region. We assign the feature in Figure 4 as the nitrogen hyperfine coupling of a nitrogenous ligand to the Cu(I). The most obvious nitrogenous candidates are one or more of the histidine ligands of the Cu.

Perturbations from Mutations at the I289 Site. The I289V mutation, although not at a copper ligand, somewhat altered the electronic structure of the Cu(I)NONiR complex, as shown by the comparison of the EPR spectra in Figure 5A (Cu(I)^{14}NONiR−wild type) and 5B (Cu(I)^{14}NONiR−I289V). The EPR spectrum of the I289A derivative, provided in Supporting Information Figure 3S, was weak and grossly distorted from the spectra of the Cu(I)NONiR derivative of wild-type NiR or I289V and showed little evidence for copper or nitrogen hyperfine coupling. Local structural information related to mutation at the I289 site is provided by ENDOR, which identifies a proton-related, mutation-induced change in the environment near the Cu(I)NO center. Figure 6 compares proton ENDOR spectra of the Cu(I)^{14}NONiR−wild type complex in protonated (6A) or deuterated solvent (6B) with the spectra of the protonated Cu(I)^{14}NONiR−I289V (6C) and the protonated Cu(I)^{14}NONiR−I289A (6D). The non-exchangeable proton features, **a** and **a′**, with hyperfine coupling of 3.0 ± 0.2 MHz, were significantly altered by the I289V and I289A mutations. The proton ENDOR spectrum of I289A had approximately the shape of the spectrum of I289V, with none of the hyperfine details (features **a** and **a′**) exhibited by wild-type protein. Because the I289V structural change to the overall protein is an extremely localized perturbation[13] occurring 4−5 Å from the Type 2 copper, a straightforward implication of these EPR and ENDOR findings is that the paramagnetic center associated with Cu(I)NONiR is near

(30) Sojka, Z.; Che, M.; Giamello, E. *J. Phys. Chem. B* **1997**, *101*, 4831−4838.
(31) Umamaheswari, V.; Hartmann, M.; Poeppl, A. *J. Phys. Chem. B* **2005**, *109*, 10842−10848.

Table 1. Comparison of *g*-Values and Cu and NO-Nitrogen Hyperfine Couplings (in MHz) from {CuNO}^{11} in Cu(I)NONiR, Nitrogenous Models, and Zeolite

complex	g_x	g_y	g_z	$^{Cu}A_x$	$^{Cu}A_y$	$^{Cu}A_z$	$^{NO}A_y$	$^{NO}A_x$	ref
Cu(I)NONiR	2.046[a]	1.998[a]	1.926[a]	102[b] (37)[c]	124[b,d] (44)[c]	238[b,d] (88)[b,c]	$^{14}A_y = 80$ (29)[b,c] $^{15}A_y = 113$ (40)[c]	$^{14}A_x = 46$ (17)[b,c,e] $^{15}A_x = 65$ (24)[c,e]	this work
1-^{14}NO	1.99	1.99	1.83	187	187	322	$^{14}A_y = 79$ $^{15}A_y = 111$	*f* *f*	ref 8
2-^{14}NO	2.00	2.00	1.84	184	184	322	$^{14}A_y = 84$ $^{15}A_y = 114$	*f* *f*	ref 8
Cu-NO/ZSM-5	1.999	2.003	1.889	449	435[g]	545[f,g]	$^{14}A_y = 87$	*h*	ref 30

[a] These *g*-values were used in fitting the X-band spectra of Figure 3. A separate estimate of *g*-values made from Q-band data (Supporting Information) gave g_x, g_y, $g_z = 2.044 \pm 0.003$, 1.998 ± 0.002, 1.923 ± 0.005. [b] Uncertainties in Cu and N hyperfine parameters are ±8 MHz or ±3 Gauss. [c] Numbers in parentheses are hyperfine couplings in Gauss. [d] Best fit of experimental spectrum occurred when $^{Cu}A_z$ and $^{Cu}A_y$ were rotated by 20° from g_z and g_y. [e] $^{NO}A_z$ was not resolved at X-band and appears to have a value less than 27 MHz or 10 Gauss. [f] $^{NO}A_x$ and $^{NO}A_z$ were not resolved for these complexes. [g] Best fit of experimental spectrum occurred when $^{Cu}A_z$ and $^{Cu}A_y$ were rotated by 40° from g_z and g_y. [h] $^{NO}A_x$ and $^{NO}A_z$ were not experimentally resolved for this complex.

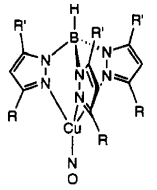

1 (R = *t*-Bu, R' = H)
2 (R = R' = Ph)

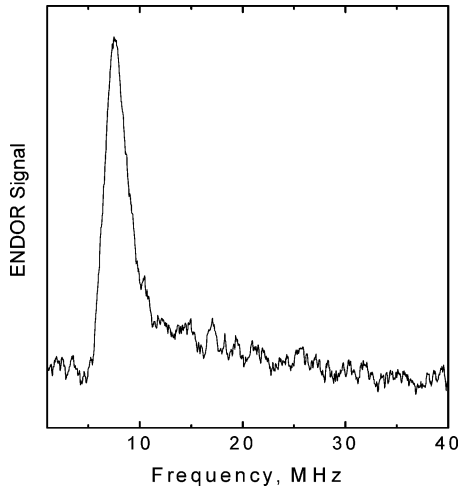

Figure 4. ENDOR from Cu(I)^{14}NONiR of wild-type NiR in a frequency region where ligand nitrogen ENDOR is normally found. This feature was not altered when ^{15}N-nitrite was used to make Cu(I)^{15}NONiR. The conditions for data collection were adiabatic rapid passage, $T = 2$ K, microwave power = 0.1 μW, 100 kHz field modulation = 0.2 mT ptp, a system time constant = 160 ms, radio frequency power ≈ 20 W, radio frequency sweep rate = 2 MHz/s, overall signal averaging time = 2000 s, $\nu_{EPR} = 34.10$ GHz, magnetic field 1.2275 T, $g = 1.985$. Radio frequency power was pulsed with a 100/900 μs duty cycle.

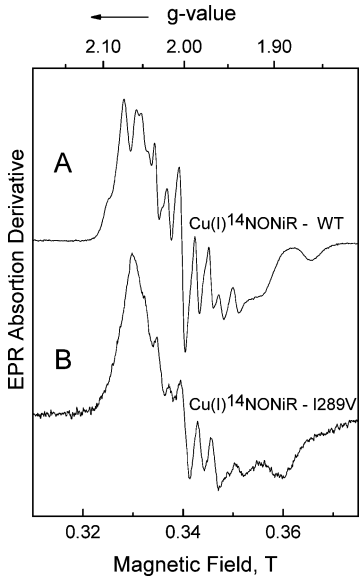

Figure 5. X-band EPR spectra of the Cu(I)NO complex of (A) Cu(I)^{14}NONiR−wild type and the corresponding complex of (B) Cu(I)^{14}NONiR−I289V mutant. Both samples were prepared as described in the Materials section using ^{14}N-nitrite with Cu in natural isotopic abundance. Sample A was contained in a larger X-band 200 μL tube, while sample B was contained in a smaller 50 μL Q-band tube. The spectra were recorded at $T = 15$ K, 0.6 mT field modulation, 100 s signal averaging over 70 mT sweep, 2 mW microwave power, EPR frequency = 9.525 GHz.

I289. Details of the proximity of the NO and I289 are provided in the Discussion.

Discussion

Molecular Orbital Scheme for the Cu(I)NO Complex of NiR. We interpreted the electronic structure of the Cu(I)NO system by a molecular orbital scheme (Scheme 2) originally due to the extended Hückel calculations reported by Hoffmann et al.[32] Although more modern DFT treatments have been used to predict the electronic and physical structure of Cu(I)NO complexes in zeolites,[33] in the model {CuNO}^{11} system of Ruggiero et al.,[8] and most recently in models of Type 2 copper in NiR,[9] the Hoffmann molecular orbital scheme works in a simple, heuristic way to explain the basic nature of the Cu(I)-NO complex and its LUMO and SOMO. In this molecular orbital scheme, the nitrosyl group is reduced to its essentials, a donor lone pair, *n*, on the nitrogen and a pair of higher lying acceptor 2p π^* orbitals. The metal 3d orbitals are filled for Cu(I), and there is a higher lying unfilled metal 4s orbital. The energies of the 3d orbitals are stabilized by back-bonding with the π^*

(32) Hoffmann, R.; Chen, M. M. L.; Elian, M.; Rossi, A. R.; Mingos, D. M. P. *Inorg. Chem.* **1974**, *13*, 2666−2675.

(33) Pietrzyk, P.; Piskorz, W.; Sojka, Z.; Broclawik, E. *J. Phys. Chem. B* **2003**, *107*, 6105−6113.

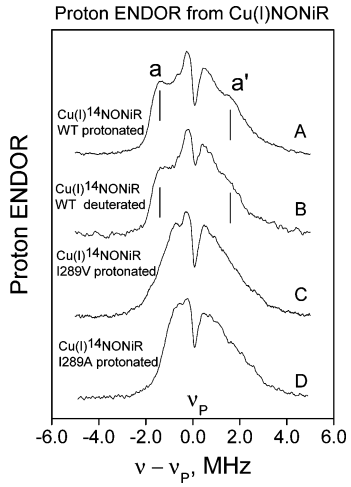

Figure 6. Proton Q-band ENDOR for (A) Cu(I)^{14}NONiR of wild-type NiR in *protonated* solvent, (B) Cu(I)^{14}NONiR of wild-type NiR in *deuterated* solvent, (C) Cu(I)^{14}NONiR of I289V in *protonated* solvent, and (D) Cu(I)^{14}NONiR of I289A in *protonated* solvent, all at a magnetic field 1.227 T ($g = 1.986$). Proton ENDOR features center at the free proton NMR frequency, which is $\nu_P = 52.23$ MHz. The conditions for data collection were adiabatic rapid passage, $T = 2$ K, microwave power = 0.22 nW, 100 kHz field modulation = 0.1 mT ptp, $\nu_{EPR} = 34.10$ GHz. Radio frequency power was pulsed with a 100/900 μs duty cycle. The features labeled **a** and **a′** have a splitting of 3.0 ± 0.2 MHz. They are significantly altered or eliminated by the I289V and I289A mutations.

Scheme 2. (Left) Energy Levels, d-Orbitals, and Spin Population of Cu(I); (Center) Perturbed d-Orbitals and Wave Functions after Bonding to NO and Bending of the Cu−N−O Bond;[a] and (Right) Important Orbitals of the Nitrosyl Ligand

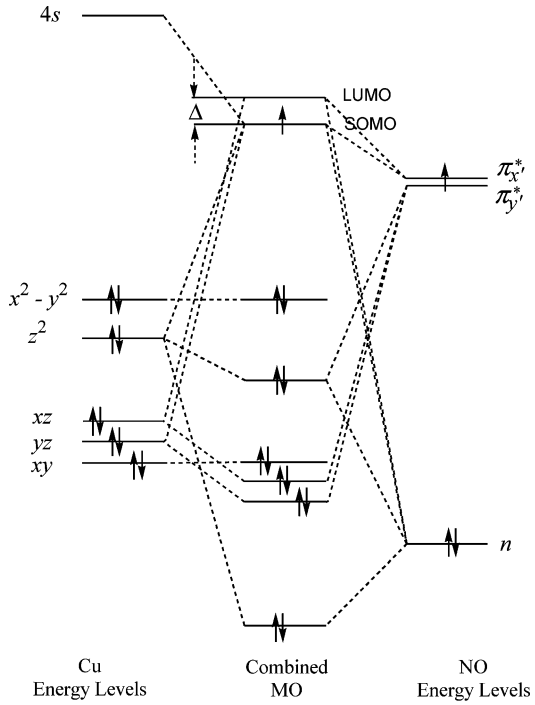

[a] The energy levels are qualitative. The lowest energy orbital has primarily *n* character, the next five orbitals have primarily d character, the next two higher energy levels have primarily π^* character, and the metal 4s orbital lies above them. The perturbation due to bending removes the degeneracy of the π^* orbitals by an energy Δ. The SOMO is designated as $\pi^*_{y'}$, although it does contain an admixture of nitrosyl and metal orbitals.

orbitals and destabilized by antibonding with the *n* orbital. There is also the potential for back-bonding interaction of the NO orbitals with the metal 4s orbital. To account for the free radical

Scheme 3. Overlap of the Cu d(z^2) and d(yz) Orbitals with the NO $\pi^*_{y'}$ and Lone Pair *n* Orbitals To Give the SOMO[a]

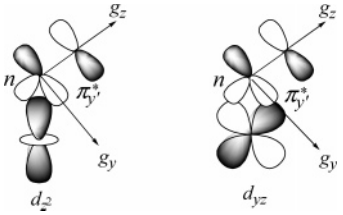

[a] The expected **g**-tensor directions for g_z (g_{min}) is along the NO bond, and g_y (g_{inter}) is perpendicular to the NO bond in the plane of CuNO. The expected direction for g_x (g_{max}) is perpendicular to the CuNO plane.

character of the complex, the π^* orbitals of NO are taken to lie higher in energy than the metal 3d orbitals, and the SOMO, which is the highest singly filled molecular orbital containing the unpaired electron, is designated as $\pi^*_{y'}$. When the CuNO bond bends, as shown in Scheme 3, the $\pi^*_{y'}$ orbital will interact more strongly with the d(z^2) orbital and less strongly with the d(yz) orbital, and the destabilizing interaction of the *n* orbital with the d(z^2) orbital will be diminished. The $\pi^*_{x'}$ orbital, perpendicular to the $y'-z'$ plane, will continue to back-bond with the d(xz) orbital as the bond bends. The result of the bending is that the degeneracy of the $\pi^*_{y'}$ and the $\pi^*_{x'}$ orbitals is removed, so that the former becomes the SOMO and the latter the LUMO; the $\pi^*_{y'}-\pi^*_{x'}$ splitting, as shown in Scheme 2, is Δ. The detailed bending, the makeup of the SOMO and LUMO, and the value for Δ will depend on the energies of d(xz), d(yz), and d(z^2) relative to the *n* and π^* orbitals of the NO.

The molecular orbital picture in Scheme 2 shows that bending away from a linear CuNO configuration will lift the degeneracy of the $\pi^*_{y'}$ and $\pi^*_{x'}$ orbitals[30] by an energy splitting Δ. For Cu(I)-NO in zeolites, Δ has been estimated from g_z-value perturbation to be in the range from 0.2 to 0.75 eV.[30] The spin−orbit coupling (by L_z) about the NO axis is predicted to couple the $\pi^*_{y'}$ and $\pi^*_{x'}$ states, and for EPR purposes this coupling leads to a significant diminishment of g_z (g_{min}) below 2.00.[30,34] Specifically,

$$g_z = 2.00 - 2\lambda/(\lambda^2 + \Delta^2)^{-1/2} \qquad (4)$$

where λ is the spin−orbit coupling constant ($\lambda = 0.015$ eV for nitrogen[35]) and Δ is the $\pi^*_x-\pi^*_y$ splitting. For Cu(I)NONiR, $g_{min} = 1.926$ and $\Delta = 0.41$ eV. For the {CuNO}^{11} biomimetic model of Ruggiero et al.,[8] $g_{min} = 1.83$ and $\Delta = 0.18$ eV. The same theory, which only considers angular momentum on the NO, predicts g_x and g_y to be essentially 2.00. However, it is possible that a Cu-centered spin−orbit coupling between the Cu d-electron components of the SOMO and the filled, lower-lying d orbitals could cause g_x (g_{max}) to be greater than 2.00.

In analogy with the findings on other {CuNO}^{11} complexes,[8,30,33] the SOMO which gives rise to the EPR signal is expected to have π^* character, with considerable unpaired spin in the 2pπ^* orbitals on the N and the O, and it could have some admixture of the *n* non-bonding orbital. It will have metal d(yz) and d(z^2) character and 4s character, where the exact amounts of metal character will depend on the energetic proximity and the overlap of the π^* and metal orbitals.

(34) Primet, M.; Che, M.; Naccache, C.; Mathieu, M. V.; Imelik, B. *J. Chim. Phys. Phys.-Chim. Biol.* **1970**, *67*, 1629−1635.
(35) Lunsford, J. H. *J. Phys. Chem.* **1968**, *72*, 2141−2144.

NO Character of the SOMO. We have obtained estimates of the hyperfine tensor for the ^{14}N and ^{15}N of the NO from the fit of our EPR data, and we find that the largest and best-resolved nitrogen features, $^{14}A_y$ or $^{15}A_y$ in Table 1, occur at $g_y = g_{inter} \approx 2.00$. The implication is that the tensor direction for g_{inter} is along the $2p\pi^*_{y'}$ orbital shown in Scheme 3. For all the {CuNO}^{11} systems (in zeolites, biomimetic models, or CuNO-NiR), this intermediate g-value is the g-value where the largest, and for several entities the only, NO nitrogen hyperfine couplings are seen. According to Table 1, the ^{14}NO nitrogen couplings, $^{14}A_y$, from all {CuNO}^{11} systems are comparable and are in the range 80−87 MHz for ^{14}NO. Like our system, the {CuNO}^{11} in ZSM-5 zeolite had an experimental ^{14}N hyperfine coupling of 84 MHz at g_y,[30] and high-level DFT calculations that included the necessary inner electron and core polarization terms for proper prediction of hyperfine couplings were done on that zeolite system.[33] The DFT calculation which accounted for the NO couplings in ZSM-5 zeolite predicted 58% of an unpaired spin (primarily in the $\pi^*_{y'}$ orbital) on the NO nitrogen, while a previous simpler molecular orbital approach on the same system had predicted ∼55% spin on the NO. A calculation of spin densities on the NO nitrogen of Cu(I)NONiR, based on standard molecular orbital theory, is explicitly presented in the Supporting Information, and the results of this calculation provide an estimate of 53% unpaired spin on the NO nitrogen of Cu(I)NONiR.

Cu Character of the SOMO. The isotropic Fermi Cu coupling, obtained from the average of all three Cu couplings for Cu(I)NONiR, is 155 MHz. This isotropic coupling is substantially smaller than that observed for the other {CuNO}^{11} complexes, which was 232 MHz for the nitrogenous biomimetic model and 476 MHz for ZSM-5 zeolite. The difference in isotropic couplings may reflect different contributions of direct 4s spin involvement and inner s shell core polarizations. An earlier molecular orbital treatment estimated 10% Cu 4s character to the {CuNO}^{11} center in the ZSM-5 zeolite, so that if the 4s contribution scales as the Cu isotropic coupling, one would expect ∼3% Cu 4s character for Cu(I)NONiR. The difference between $^{Cu}A_z$ and $^{Cu}A_y$ is due to dipolar contributions from Cu 3d electron density, and this difference ranges from 110 to138 MHz for the {CuNO}^{11} complexes in Table 1. For {CuNO}^{11} in ZSM-5 zeolite, the $^{Cu}A_z - {}^{Cu}A_y$ difference was due to unpaired electron spin in the d(z^2) and d(yz) orbitals; the total 3d contribution was about 10%, where ∼8% was in the d(z^2) orbital and ∼2% was in the d(yz).[30,33] A calculation after Sojka et al.,[30] based on our empirical estimates of Cu hyperfine couplings for Cu(I)NONiR, yielded Cu d(z^2) and d(yz) spin densities and is presented in the Supporting Information. This calculation indicated for wild-type Cu(I)NONiR a total 3d spin population of 14%, where 10.5% was in the d(z^2) orbital and 3.5% was in the d(yz) orbital. A total metal spin contribution of 17% thus resulted from adding the 14% 3d contribution and the 3% 4s contribution.

It is noteworthy that, if the NO were ligated in a side-on fashion to the copper, as has been reported for the Cu(II) system described by Tocheva et al.,[5] one would expect that the $\pi^*_{y'}$ orbital of the NO, whose direction determines g_{inter}, would maximally overlap the copper d(z^2) orbital, as shown in Scheme 3. Electron spin would be directed preferentially into the d(z^2) orbital, so that the maximal dipolar contribution to the Cu hyperfine coupling would be at the g_{inter} (g_y) g-value rather than the g_{min} (g_z) g-value. The maximal Cu hyperfine coupling is *not* found at g_{inter} but at g_{min}, and the implication is that the NO of Cu(I)NONiR is not bound side-on. In fitting the EPR spectra in Figure 3, we included the rotation of the $^{Cu}A_z$ and $^{Cu}A_y$ components of the **A**-tensor with respect to the g_z and g_x components of the **g**-tensor. Such a rotation implies that the Cu−N−O bond angle is rotated by 20° away from a linear 180° angle. That 20° rotation would predict a Cu−N−O bond angle of ∼160°, which is consistent with the Cu−N−O bond angle of 163.4° obtained crystallographically from the nitrogenous biomimetic {CuNO}^{11} complex reported by Ruggerio et al.[8]

Weak Nitrogen Hyperfine Coupling Implies Histidine Ligation to Cu(I). As pointed out in the Results section relevant to Figure 4, there are no naturally occurring nuclei for Cu(I)-NONiR other than ^{14}N-nitrogen which will provide Q-band ENDOR features in the frequency region from 1 to 15 MHz. Thus, the feature in Figure 4 was assigned as nitrogen hyperfine coupling. The NO is ligated to copper, there is spin density on the copper, and the copper in turn has histidine ligands. The most obvious candidates for the feature in Figure 4 are therefore one or more of the histidine nitrogen ligands of the Cu.[36] If the ENDOR feature is the $^{14}\nu^+_{ENDOR}$ feature of ^{14}N, with $^{14}\nu =$ 3.93 MHz at 1.275 T (eq 3), its hyperfine coupling would be about 7.2 MHz. Such a hyperfine coupling is less, by 3−5 times, than those nitrogen hyperfine couplings observed from histidine ligands of cupric Type 2 copper in resting NiR.[11] For copper complexes, the hyperfine coupling with a liganding nitrogen primarily arises from σ-type overlap of nitrogen 2s and 2p electrons in an sp^n orbital with copper d orbitals. For example, the average hyperfine coupling to liganding porphyrin nitrogens of CuTPP is 47 MHz,[37] and the nitrogen 2s plus 2p spin density on each pyrrole nitrogen of CuTPP is ∼9.5%, with a ratio of 2p to 2s slightly larger than 2. The nitrogen orbitals of CuTPP antibond with the Cu d(x^2-y^2). A rough estimate of the spin density on the histidine of Cu((I)NONiR can be obtained if, using the CuTPP information, we scale the spin density proportionally to the average nitrogen hyperfine coupling. The coupling of 7.2 MHz would then correspond to roughly 1.4% of an unpaired electron spin on a ligand nitrogen. It is conceivable that such electron spin would be transferred from the NO through the copper d(z^2) orbital to an opposite, i.e., trans, histidine ligand.

Information from Mutations at the I289 Site. The I289V mutation, which eliminated the Cδ1 methyl group of I289, showed a changed EPR spectrum (Figure 5A versus 5B) and a changed proton ENDOR spectrum (Figure 6A,B versus 6C). Yet this I289V mutation is a highly conservative mutation, as shown by its crystallographic structure.[13] This mutation leads to no global structural perturbation and does not perturb any catalytically essential residue other than 289.[13] Thus, the

(36) Although we looked for larger couplings which could be assigned to the NO itself, these have not been observed. We point out that ENDOR is a non-linear process whose success at resolving nuclear hyperfine features coupled to an electron spin depends on a compendium of relaxation processes (Feher, G.; Gere, E. A. *Phys. Rev.* **1956**, *103*, 501). Thus, one cannot expect ENDOR always to resolve couplings that are observed by EPR, and negative ENDOR results need not be meaningful. For example, large EPR-resolved couplings of the six-coordinate heme−^{15}NO in cytochrome *c* oxidase (∼65 MHz in magnitude and comparable to those seen by EPR of Cu(I)NONiR) are not resolved by ENDOR (LoBrutto, R.; Wei, Y. H.; Mascarenhas, R.; Scholes, C. P.; King, T. E. *J. Biol. Chem.* **1983**, *258*, 7437−7448.)

(37) Brown, T. G.; Hoffman, B. M. *Mol. Phys.* **1980**, *39*, 1073−1090.

spectroscopic changes we observed for I289V reflect a localized structural change rather than a delocalized distortion that might extend, for example, to Cu−His ligands. The EPR result indicates that the Cδ1 methyl group influences the electronic structure of Cu(I)NONiR, as evidenced by *g*-values and hyperfine structure. The proton ENDOR features denoted by **a** and **a′** in Figure 6 A,B occur for wild-type protein but are significantly altered or eliminated for the I289V and I289A mutants. The most direct assignment for these features and their behavior is the Cδ1 methyl protons of I289, which are close enough to the NO paramagnetic center to cause the ∼3.0 MHz proton coupling of features **a** and **a′**. For the mutants, this coupling is eliminated along with the Cδ1 methyl.

The 3.0 MHz coupling of **a** and **a′** is associated with spin-proton coupling by using the dipolar formula (eq 2). Here, the spin density in the delocalized Cu(I)NONiR wave function will be greatest at the nitric oxide N but delocalized over N, O, and Cu.[38] The dipolar formula includes the angle θ between the applied magnetic field and the vector from the proton to the electron spin; if $\theta = 90°$, a coupling of 3.0 MHz implies a spin−proton distance of 3.0 Å, and if $\theta = 0°$, it implies a spin−proton distance of 3.7 Å. In previously reported structures, the distance from the axial ligand of Type 2 Cu in NiR to Cδ1 methyl and Cγ1 methylene protons of I289 averaged 3.6 Å, with the closest protons 2.8−2.9 Å away. (See details of distance computation in footnote 39.) The average distance from the axial ligand to the Cγ2 methyl protons is 4.0 Å, with the closest Cγ2 proton at 3.2 Å. The Cβ proton is 5.3 Å distant. The 3.0−3.7 Å distances implied by ENDOR would thus be consistent with those distances estimated between an axial ligand of Type 2 Cu and the Cδ1 methyl, the Cγ1 methylene, or perhaps one Cγ2 proton of I289. The proton ENDOR results are not consistent with a dipolar coupling between spin localized, instead, on the more distant copper and the protons on I289, which would imply a coupling <1.5 MHz to the I289 protons.

The similarity of the ENDOR line shapes of I289V (Figure 6C) and I289A (Figure 6D) implies that the Cγ protons of I289V have little effect on the proton ENDOR line shape because that line shape persists when Val is replaced by Ala. If the Cγ protons of I289 and V289 have the same location, additional evidence is thereby provided that the Cδ1 methyl protons of I289, rather than the Cγ protons of I289, will account for the features **a** and **a′** in Figure 6A,B. The conclusion from EPR is that non-covalent interaction with the bulky I289 side chain is important in establishing the electronic structure of the Cu(I)-NONiR. The conclusion from ENDOR is that the I289 Cδ1 methyl proton hyperfine couplings assigned to features **a** and **a′** serve to locate the NO, which carries the electron spin. They locate the NO as an axial ligand to Type 2 copper in the space between the Cu and the Cδ1 methyl protons of I289.

(38) This necessarily imprecise location of the spin does not interfere in our ultimately locating the position of the spin on the NO within 3.0−3.7 Å of the Cδ1 and Cγ1 protons of I289.

(39) Since there are no crystal structures of Cu(I)NONiR, we have used the water oxygen of the NiR aquo derivative (ref 3) or the N of the recent Cu(II)NO derivative (ref 5) to estimate distances to protons of I289 from the axial ligand positioned on Type 2 copper. The latter Cu(II)NO derivative described by Tocheva et al.[5] is not our derivative, but at least it provides a reference point for estimating distances from N of NO to nearby I289 protons. Protons were placed on isoleucine carbons with the rectification tool of ChemPro because protons are not resolved by X-ray crystallography.

Conclusions

Copper-containing nitrite reductase endogenously produces its own NO from nitrite under reducing conditions, and the comparison between the EPR signals that were respectively produced from ^{14}N- versus ^{15}N-nitrite (spectrum 2A versus 2B) provided evidence that endogenously produced NO is a major component of the paramagnetic signal of Cu(I)NONiR. The marked similarity of the signals (spectrum 1A versus 1C) from endogenously produced ^{14}NO and from exogenous ^{14}NO gas added anaerobically in a limited amount was additional evidence that NO is a component of the paramagnetic signal of Cu(I)-NONiR. Comparison of the well-resolved nitrogen coupling near $g = 2.00$ to those of other {CuNO}^{11} systems on which DFT treatments have been performed indicates 50−55% unpaired spin of Cu(I)NONiR exists in the 2p orbitals of the NO nitrogen. The evidence for copper in Cu(I)NONiR is directly shown by the change in its EPR spectrum (spectrum 2C) when the NiR was prepared with isotopically enriched ^{63}Cu, as opposed to Cu in natural abundance. There is a similarity of *g*-values from Cu(I)NONiR, notably the unique $g_z < 2.00$, to *g*-values from NO trapped in matrices or absorbed on surfaces,[34,35,40] but the copper hyperfine structure associated with g_z is another indicator that the complex we have designated Cu(I)NONiR does contain copper. Using theory developed by Sojka et al.,[30] we have estimated the total unpaired spin on the copper d and 4s orbitals to be ∼17%. Assuming that the contributions of the Cu, N, and O sum to unity, this would mean that the oxygen of the NO should have ∼30% unpaired spin. There is, in addition, ENDOR evidence that Cu(I)NONiR has at least one nitrogenous ligand, most likely histidine, with ∼1% unpaired spin. The perturbation to the EPR spectrum (Figure 5) and to the proton ENDOR spectrum (Figure 6) from the I289V and I289A mutations, which eliminate the Cδ1 methyl, is a sign that the paramagnetic NO center associated with Cu(I)NONiR is near I289. The proton hyperfine coupling indicated that the electron spin which interacts with the protons of I289 is centered 3.0−3.7 Å away from the bulky Cδ1 and Cγ side chains of I289. This distance is consistent with the electron spin primarily being on the axial NO ligand to Type 2 copper, while the NO abuts the bulky I289 side chains, most likely the Cδ1 methyl group. In short, the system which we report here and spectroscopically characterize is a Cu(I)NO system localized on NO but situated sufficiently near to the original Type 2 copper that it covalently interacts with that copper. Additionally, the NO experiences a non-covalent perturbation by the bulky side chain of nearby I289.

Acknowledgment. These studies were partially supported by the NIH (EB00326929, C.P.S.) and the DOE (95ER2-0206, J.P.S.). We are grateful to Dr. William Antholine for providing isotopically enriched ^{63}Cu and for providing the original spectra of the model Cu(I)NO complexes reported by Ruggiero et al.[8] and preliminary S-band spectra of Cu(I)-NONiR.

Supporting Information Available: Figure 1S, the Q-band first derivative EPR spectrum of Cu(I)^{14}NONiR; Figure 2S, comparing the X-band spectra of Cu(I)^{14}NONiR (2SA) and Cu(I)^{15}NONiR (2SB) with the corresponding ^{14}NO and ^{15}NO

(40) Lunsford, J. H. *J. Catal.* **1969**, *14*, 379−385.

derivatives of the Cu(I)NO model compounds described by Ruggiero et al.;[8] Figure 3S, comparing the EPR spectra from Cu(I)NONiR prepared from I289V and I289A; a calculation of spin densities on the NO nitrogen of Cu(I)NONiR based on standard molecular orbital theory; and a calculation of Cu d(z^2) and d(yz) orbital coefficients via methods of Sojka et al.[30] This material is available free of charge via the Internet at http://pubs.acs.org.

JA056166N